Sensors and Materials, Vol. 36, No. 1 (2024) 163–168
MYU Tokyo

S & M 3506

Effective Volume of TlBr Semiconductor Detector

Sota Hasegawa,[1*] Kenichi Watanabe,[1] Yusuke Sugai,[1]
Mitsuhiro Nogami,[2] and Keitaro Hitomi[2]

[1]Department of Applied Quantum Physics and Nuclear Engineering, Kyushu University,
744 Motooka, Nishi-ku, Fukuoka 819-0395, Japan
[2]Department of Quantum Science and Energy Engineering, Tohoku University,
Aoba, Aramaki, Aoba-ku, Sendai 980-8579, Japan

(Received August 31, 2023; accepted January 18, 2024)

Keywords: TlBr semiconductor detector, effective volume, small-pixel effect

TlBr semiconductor detectors are candidate high-detection-efficiency, high-energy-resolution, and room-temperature gamma-ray spectrometers. We evaluate the effective volume of a small-anode TlBr detector with a guard electrode through basic experiments and simulations, which are conducted for various voltages applied to the guard electrode. We confirm that the detection efficiency increases with decreasing guard voltage compared with the anode and saturates at a certain value. Under saturation conditions, the effective volume is evaluated to be 56% by simulation. In addition, we experimentally confirm that the energy resolution can be improved for a small-anode TlBr detector with a guard electrode by correcting the signal pulse height by pulse shape discrimination.

1. Introduction

TlBr semiconductor detectors are expected to be used as gamma-ray spectrometers with high detection efficiency, high energy resolution, and room-temperature operation.[1-10] Since TlBr is composed of elements with high atomic numbers (Tl = 82, Br = 35) and has a high density of 7.56 g/cm^3, it is expected to show high detection efficiency. In addition, TlBr has a wide bandgap of 2.68 eV, which allows it to operate at room temperature. Owing to improvements in the material purification process,[11] relatively high mobility–lifetime ($\mu\tau$) products have been achieved. As a result, such detectors can exhibit an excellent energy resolution of about 1% for gamma rays of 662 keV.[4–10]

In TlBr, the mτ product of holes is lower than that of electrons, unlike Si or Ge. Therefore, to achieve a high energy resolution in TlBr semiconductor detectors, it is necessary to emphasize the contribution of electron migration with high mobility and high charge collection efficiency. In other words, it is necessary to apply a single-polarity charge sensing method.[12] A typical method of single-polarity charge sensing is to use the small-pixel or near-field effect. The small-pixel effect can be understood by the presence of highly nonuniform weighting potentials induced with a small-pixel electrode. The phenomenon can be explained using the Shockley–

*Corresponding author: e-mail: hasegawa.sota.637@s.kyushu-u.ac.jp
https://doi.org/10.18494/SAM4632

ISSN 0914-4935
https://myukk.org/

Ramo theorem.[13,14] However, in general, the effective volume of detectors using the small-pixel effect is complex to evaluate. This kind of consideration is important and has been investigated for detectors with hole mτ products, such as CdTe and CdZnTe, which are also expected as room-temperature semiconductor detectors. However, in addition, TlBr suffers from low electron mobility and ballistic deficit. Therefore, in this study, we investigate the effective volume of a TlBr detector using the small-pixel effect through basic experiments and simulations.

2. Simulation of Induced Signal Pulses

In this study, the effective volume is evaluated through comparisons between experiments and simulations for a TlBr detector. In these simulations, the weighted and actual electric potentials and electric fields are first calculated using the finite element method with Elmer simulation software.[15] In addition, a gamma-ray transport calculation is performed with the Monte Carlo simulation code EGS5.[16] In this calculation, the generation positions of charge carriers, such as electrons and holes, are determined. Using the information on the initial positions of charge carriers and the electric field in the crystal, we calculate the trajectories of electrons and holes with our own simulation code for charge transport. On the basis of the migration of charges, the charges induced on each electrode, that is, the signal waveforms, are calculated using the Shockley–Ramo theorem. Finally, the calculated signal waveforms are processed with the same signal processing procedure as that used in the experiments to create the signal pulse height spectrum.

3. Materials and Methods

As a single-polarity charge sensing detector, the small-anode TlBr detector with a guard electrode shown in Fig. 1 was used. The size of this detector was 5 × 5 × 5 mm^3. Tl metal electrodes were deposited on the top and bottom surfaces of a TlBr crystal. On the top surface, a guard electrode was placed around the small-anode electrode. A cathode was deposited on the entire bottom surface. The electrodes were coated with resin to prevent degradation. In a small-anode detector with a guard electrode, the anode signal is mainly induced by electron migration near the anode owing to the highly nonuniform weighting potential around the small anode.

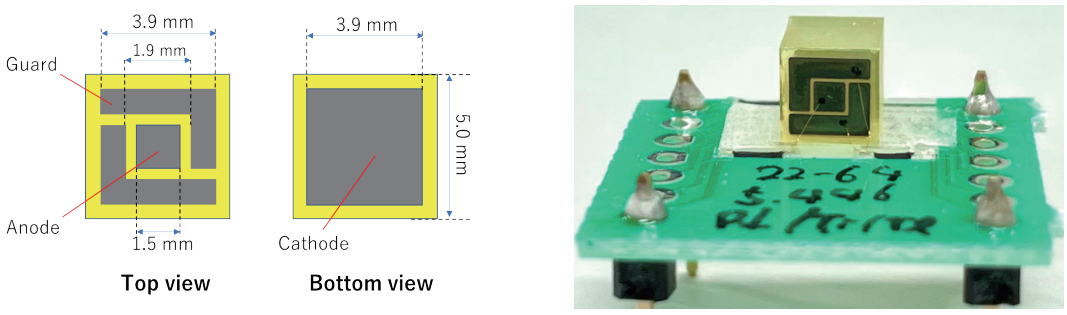

Fig. 1. (Color online) (a) Top and bottom views of 5 × 5 × 5 mm^3 TlBr semiconductor detector. (b) Photograph of the TlBr semiconductor detector used in the experiment.

The anode was grounded while a voltage of – 200 V was applied to the cathode. The effective volume was varied by changing the voltage applied to the guard electrode, as shown in Fig. 2. The anode and cathode signals were individually fed into charge-sensitive preamplifiers. The preamplifier outputs were connected to an analog-to-digital converter (Model 1819-16, Clear Pulse) to digitize the signal waveforms. The pulse waveforms were processed with the trapezoidal filter in a PC. The signal pulse heights were determined from the processed pulses. Finally, the signal pulse height spectrum was created in the PC. In this experiment, a Cs-137 gamma-ray source, which emitted 662 keV gamma rays, was used.

4. Results and Discussion

Figure 3 shows the signal pulse height spectra obtained from the small-anode TlBr detector with a guard electrode when irradiating the detector with 662 keV gamma rays from Cs-137. As examples, the pulse height spectra are shown for guard voltages of 0, −50, and −100 V. The measurement time was 300 s in all cases. It can be seen that the detection efficiency increases with decreasing guard voltage. On the other hand, the peak resolution deteriorates with decreasing guard voltage. The degradation of the resolution could be caused by an increase in leakage current between the anode and guard electrodes. It could also be due to the variation in charge collection efficiency caused by the difference in electron transport trajectory. In addition,

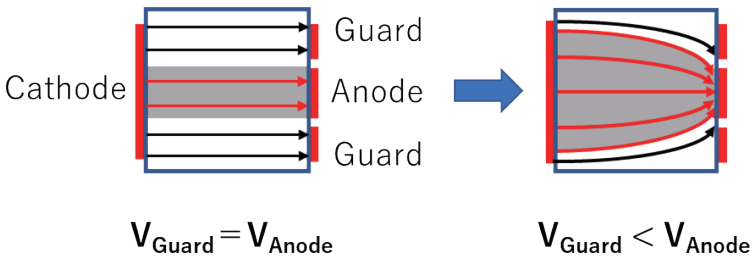

Fig. 2. (Color online) Conceptual drawing of electric field lines in the small-anode TlBr detector with a guard electrode. The left and right figures show the cases of $V_{Guard} = V_{Anode}$ and $V_{Guard} < V_{Anode}$, respectively. The arrows represent electric field lines. The gray areas indicate the effective volume of the detector.

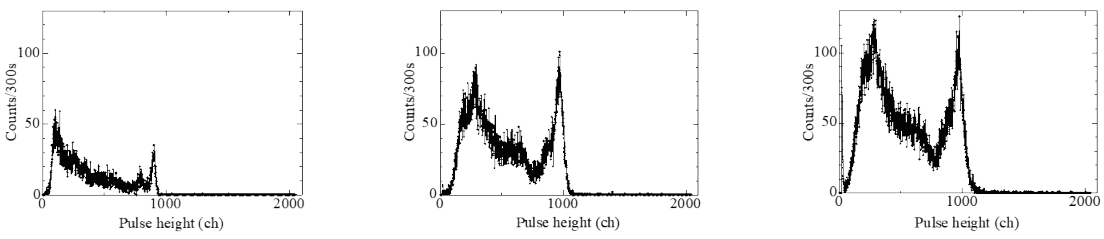

Fig. 3. Experimental pulse height spectra obtained for guard voltages of (a) 0, (b) −50, and (c) −100 V. In all cases, the anode and cathode voltages were 0 and −200 V, respectively.

simulations of the small-anode TlBr detector with a guard electrode were performed under the same conditions as the experiments. Figure 4 shows the signal pulse height spectra obtained from the simulations. The simulation results are in good agreement with the experimental results. Figure 5 shows the guard voltage dependence of the absolute peak efficiency. Both the experimental and simulation results are plotted. Although there are some differences in the absolute values of the efficiency, the experiments and simulations show similar trends, with the peak efficiency gradually increasing with decreasing guard voltage and saturating around −100 V. The difference in absolute efficiency can be attributed to the small difference in experimental geometry.

We evaluated the effective volume of the detector by simulation. Figure 6 shows the spatial dependence of the charge collection efficiency on the position of charge carrier generation in the small-anode detector with a guard electrode. When the guard voltage is equal to the anode voltage, the effective volume is limited to a value below the anode voltage. We can see that the effective volume increases with decreasing guard voltage. When a voltage of −100 V is applied to the guard electrode, although almost all the volume is seen to be effective, the effective volume is 56% of the crystal. In the current electrode configuration, charges cannot be fully collected from the corners of the detector. As a result, approximately 40% of the crystal remains insensitive in this configuration.

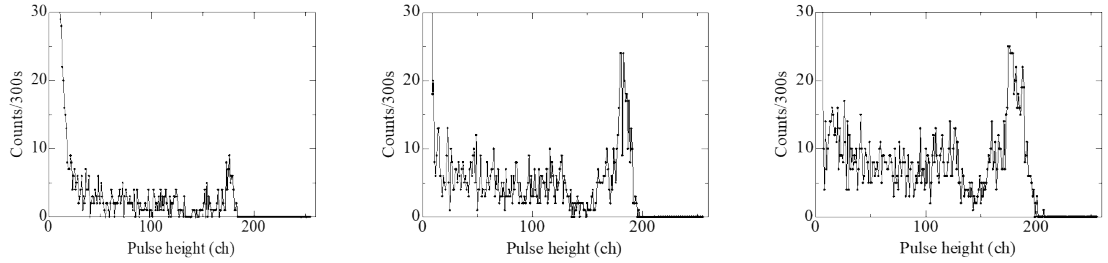

Fig. 4. Simulated pulse height spectra obtained for different guard voltages of (a) 0, (b) −50, and (c) −100 V. In all cases, the anode and cathode voltages were 0 and −200 V, respectively.

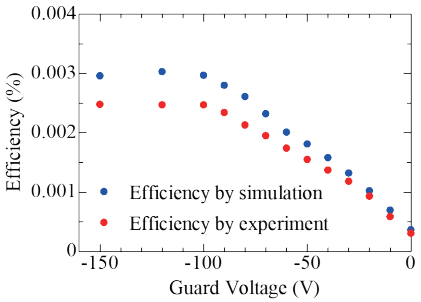

Fig. 5. (Color online) Guard voltage dependence of the absolute peak efficiency. Experimental and simulation results are plotted.

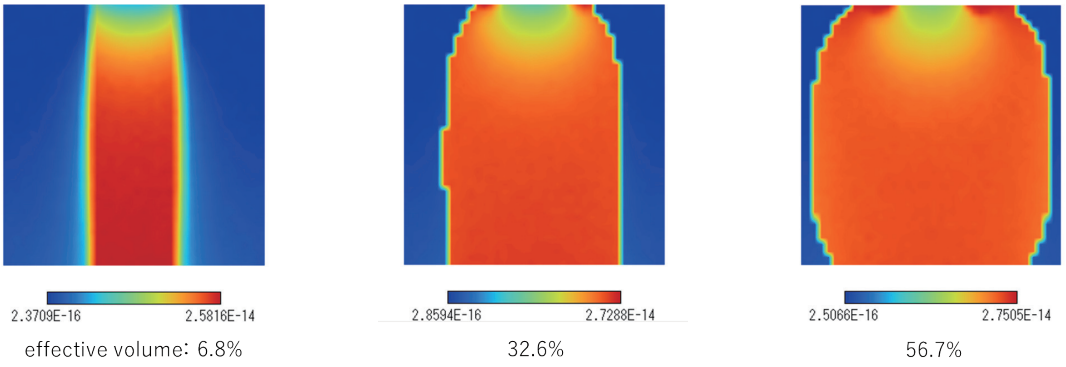

(a) (b) (c)

Fig. 6. (Color online) Spatial dependence of the charge collection efficiency on the position of charge carrier generation in the small-anode TlBr detector with a guard electrode. Guard voltages of (a) 0, (b) −50, and (c) −100 V.

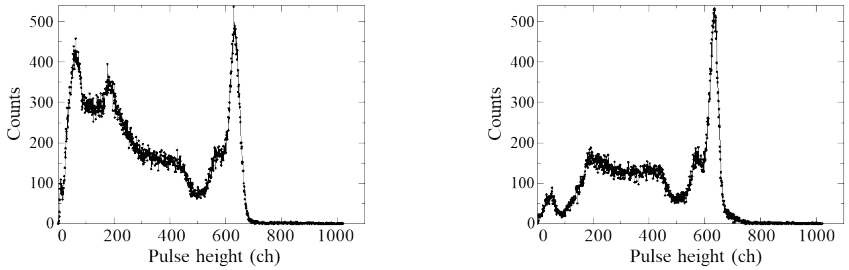

(a) (b)

Fig. 7. Signal pulse height spectra obtained before and after pulse height correction based on the rise time. In this case, the anode, guard, and cathode voltages were 0, −50, and −50 V, respectively.

In this simulation, leakage current is not considered. However, the degradation of the peak resolution with decreasing guard voltage can be observed in Fig. 4. One of the reasons for this degradation is considered to be the variation in charge collection efficiency due to the difference in electron transport trajectory. This difference results in the difference in signal pulse shape. The peak resolution can be improved by correcting the pulse height by signal pulse shape discrimination. Therefore, we attempted to correct the pulse height by pulse shape discrimination with the rise time of the preamplifier signals. The rise time was defined as the time from 5 to 90% of the peak pulse height. Figure 7 shows the signal pulse height spectra obtained before and after pulse height correction based on the rise time. In this case, the guard voltage applied was −50 V. In the corrected spectrum, the full energy absorption peak is clearly separated from the escape peak. We experimentally confirmed the improvement in peak resolution by correcting the pulse height by pulse shape discrimination. Although the signal pulse shape includes information on electron trajectories, not all information can be extracted from only the rise time. Further improvement in peak resolution can be expected by applying a more advanced signal pulse shape discrimination method.

5. Conclusions

We have investigated the effective volume of a small-anode TlBr detector with a guard electrode through basic experiments and simulations. Measurements were made for various voltages applied to the guard electrode. The detection efficiency was confirmed to increase with decreasing guard voltage and to saturate at a certain voltage of the guard electrode. In addition, the effective volume was evaluated by simulation. In the saturated case, the effective volume was evaluated to be 56%. For the current electrode configuration, it was concluded that charges cannot be fully collected from the corners of the detector. In the small-anode detector with a guard electrode, since the signal pulse shape includes information on electron transport trajectories, pulse height correction using pulse shape discrimination is expected to be effective for improving the energy resolution.

As our future work, we will attempt to apply a more advanced pulse shape discrimination method using machine learning techniques to achieve both high detection efficiency and high energy resolution.

Acknowledgments

This work was partially supported by JSPS KAKENHI Grant Number JP 22H02008. It was also partially supported by the Cooperative Research Project of Research Institute of Electronics, Shizuoka University.

References

1 K. Hitomi, T. Murayama, T. Shoji, T. Suehiro, and Y. Hiratate: Nucl. Instrum. Methods Phys. Res. A **428** (1999) 372.
2 K. Hitomi, O. Muroi, T. Shoji, T. Suehiro, and Y. Hiratate: Nucl. Instrum. Methods Phys. Res. A **436** (1999) 160.
3 T. Onodera, K. Hitomi, T. Shoji, and Y. Hiratate: Nucl. Instrum. Methods Phys. Res. A **525** (2004) 199.
4 K. Hitomi, T. Onodera, T. Shoji, and Z. He: Nucl. Instrum. Methods Phys. Res. A **578** (2007) 235.
5 K. Hitomi, T. Shoji, and Y. Niizeki: Nucl. Instrum. Methods Phys. Res. A **585** (2008) 102.
6 K. Hitomi, Y. Kikuchi, T. Shoji, and K. Ishii: Nucl. Instrum. Methods Phys. Res. A **607** (2009) 112.
7 B. Donmez, Z. He, H. Kim, L. J. Cirignano, and K. S. Shah: Nucl. Instrum. Methods Phys. Res. A **623** (2010) 1024.
8 K. Hitomi, T. Shoji, and K. Ishii: J Cryst. Growth **379** (2013) 93.
9 K. Hitomi, T. Tada, T. Onodera, S.-Y. Kim, Y. Xu, T. Shoji, and K. Ishii: IEEE Trans. Nucl. Sci. **60** (2013) 1156.
10 K. Hitomi, T. Onodera, S-Y. Kim, T. Shoji, and K. Ishii: Nucl. Instrum. Methods Phys. Res. A **747** (2014) 7.
11 K. Hitomi, T. Onodera, and T. Shoji: Nucl. Instrum. Methods Phys. Res. A **579** (2007) 153.
12 A. Owens and A. G. Kozorezov: Nucl. Instrum. Methods Phys. Res. A **563** (2006) 31.
13 W. Shockley: Currents to conductors induced by a moving point charge, J. Appl. Phys., **9** (1938) 635.
14 S. Ramo: Currents Induced by Electron Motion, Proc. IRE, **27** (1939) 584.
15 M. Malinen and P. Råback: Multiscale Modelling Methods for Applications in Material Science: Elmer finite element solver for multiphysics and multiscale problems (Forschungszentrum Jülich, 2013) p. 101.
16 H. Hirayama, Y. Namito, A. F. Bielajew, S. J. Wilderman, and W. R. Nelson: The EGS5 Code System, KEK Report 2005-8 (2005).